J Mol Model (2011) 17:633–647
DOI 10.1007/s00894-010-0749-x

ORIGINAL PAPER

Theoretical and experimental studies on the inhibition potentials of aromatic oxaldehydes for the corrosion of mild steel in 0.1 M HCl

Nnabuk Okon Eddy · Benedict I. Ita

Received: 20 December 2009 / Accepted: 7 May 2010 / Published online: 4 June 2010

Abstract Experimental aspect of the inhibition of the corrosion of mild steel by oxaldehydes was carried out using gravimetric, gasometric and thermometric methods while the theoretical studies were carried out using quantum chemical principle and quantitative structure activity relation (QSAR) approaches. The results obtained indicated that the studied oxaldehydes are good inhibitors for the corrosion of mild steel in HCl solutions. The adsorption of the inhibitors on mild steel surface is spontaneous, exothermic and is consistent with the assumptions of Langmuir adsorption isotherm. Excellent correlations were found between the calculated quantum chemical parameters and experimental inhibition efficiencies of the studied compounds. Correlations between theoretical and experimental inhibition efficiencies (for the different Hamiltonians, namely, PM6, PM3, AM1, RM1 and MNDO) were very close to unity. Condensed Fukui function and condensed softness have been used to determine the sites for electrophilic and nucleophilic attacks on each of the inhibitors.

Keywords Corrosion · Inhibition · Mild steel · Oxaldehyde · Theoretical/experimental studies

List of symbols

χ	Electronegativity
η	Global hardness
ΔE	Energy gap (i.e., E_{LUMO}-E_{HOMO})
μ	Dipole moment
σ	Chemical potential
C-C	Core core repulsion energy
Cosmo	Donductor like a screening model
CosA	Cosmo area
CosV	Dosmo volume
DFT	Density functional theory
EA	Electron affinity
EE	Electronic energy of a molecule
E_{HOMO}	Energy of the highest occupied molecular orbital
E_{LUMO}	Energy of the lowest unoccupied molecular orbital
$E_{(N-1)}$	Ground state energy of the system with N-1 electron
$E_{(N)}$	Ground state energy of the system with N electron
$E_{(N+1)}$	Ground state energies of the system with N+1 electrons
f^+	Fukui function for the nucleophile
f^-	Fukui function for the electrophile
S	Global softness
S^+	Global softness for the nucleophile
S^-	Global softness for the electrophile
IP	Ionization potential
q	Muliken or Lowdin charge
Q_{ads}	Heat of adsorption
QSAR	Quantitative structure activity relation
R	Gas constant
TE	Total energy of the molecule
AM1	Austin model 1
PM3	Parametric method number 3
PM6	Parametric method number 6
RM1	Recife model 1
MNDO	Modified neglect of diatomic overlap

N. O. Eddy (✉)
Department of Chemistry, Ahmadu Bello University,
Zaria, Kaduna State, Nigeria
e-mail: nabukeddy@yahoo.com

B. I. Ita
Department of Chemistry, University of Calabar,
Calabar, Cross River State, Nigeria

Introduction

Mild steel is highly ductile and wieldable. Therefore, it is widely used in industrial processing machinery and equipments in many industries including minerals, fertilizers, timber, oil, chemicals and modern semiconductor plants. However, the major problem associated with the use of this valuable metal is corrosion, which occurs when the metal is in contact with an aggressive medium [1–3].

In view of the high cost of protecting mild steel against corrosion attack, numerous studies have been carried out on the inhibition of the corrosion of mild steel. The results of most of the published research revealed that most of the well known inhibitors suitable for the inhibition of the corrosion of mild steel in acidic medium are heterocyclic compounds having hetero atoms in their aromatic or long carbon chain systems [4, 5]. For these compounds, their adsorption on the metal surface is the initial step for the inhibition process. Also, the presence of heteroatoms (such as N, O, P, and S) as well as triple bond or aromatic ring in their molecular structure facilitate the adsorption of the inhibitor [6]. Generally, a strong coordination bond causes higher inhibition efficiency.

Corrosion inhibition process can be regarded as a process involving donation and acceptance of electrons. In this case, the metal acts as an electrophile while the nucleophilic center is in the inhibitor [7]. There are increasing numbers of research that attempt to correlate the corrosion inhibition efficiencies of most inhibitors with quantum chemical parameters.

Semiempirical methods have been successfully applied in the correlation of experimental and theoretical inhibition efficiencies of some inhibitor [8–10]. However literature is scanty on the use of this principle for the study of the corrosion inhibition behavior of oxaldehydes for mild steel in HCl solutions. The present study is aimed at investigating the inhibitive potentials of 2-hydroxyl-1,2-di(pyridine-2-yl) ethanone (pyridoin), 2-hydroxy-1,2-diphenyl ethanone (benzoin) and benzil. The chemical and optimized structures (optimized, using B3LYP) of these compounds are presented in Fig. 1. Quantitative structure activity relation (QSAR) shall be used to derive equations for the calculation of theoretical inhibition efficiencies of the inhibitors (using quantum chemical parameters). This shall furnish information on the possibility of synthesizing inhibitors that are structurally related to the one under study. Density functional theory shall be used in the determination of the sites for electrophilic and nucleophilic attacks. Finally, theoretical and experimental inhibition efficiencies shall be correlated.

Experimental techniques

Materials

Materials used for the study were mild steel sheet of composition (wt %); Mn (0.6), P (0.36), C (0.15) and Si (0.03) and the rest Fe. The sheet was mechanically pressed cut into different coupons, each of dimension, 5×4× 0.11 cm. Each coupon was degreased by washing with

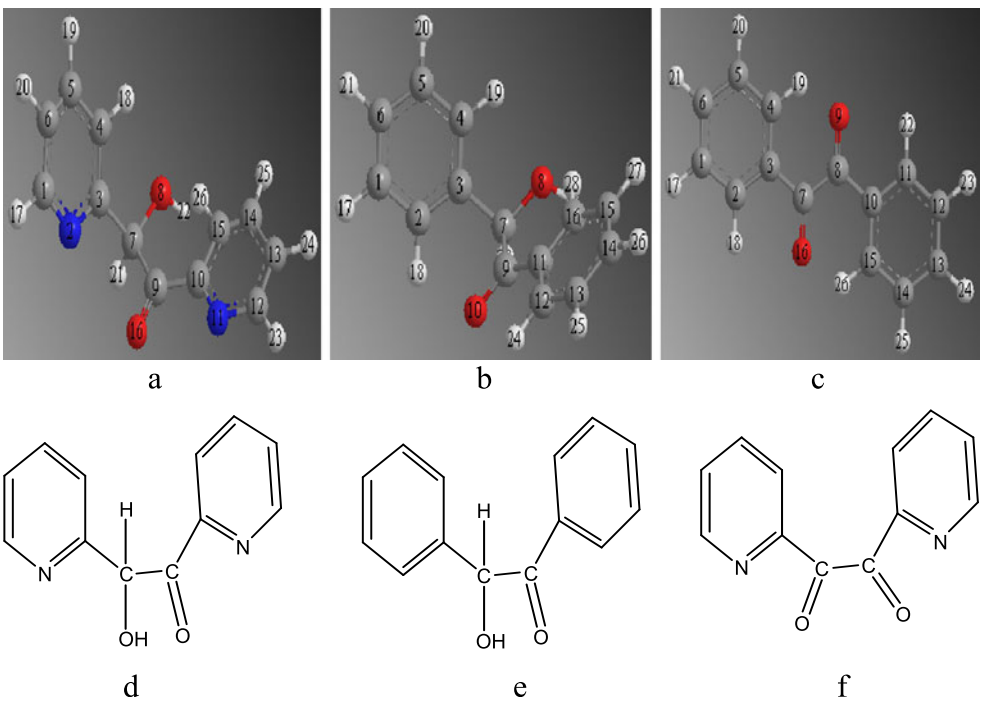

Fig. 1 Chemical and optimized structures of pyridoin (**a** and **d**), benzoin (**b** and **c**) and benzil (**c** and **f**)

ethanol, dipped in acetone and allowed to dry in air before they were preserved in a desicator. All reagents used for the study were Analar grade and double distilled water was used for their preparation.

The inhibitors were supplied by Dr. B. I. Ita of the Department of Chemistry, University of Calabar, Nigeria. They were used without further purification. The concentrations range for the inhibitors was 1×10^{-4} to 5×10^{-4}M. Each of these concentrations was dissolved in 0.1 M and 2.5 M HCl and preserved in a plastic container for use in gravimetric and gasometric experiments respectively.

Gravimetric method

In the gravimetric experiment, a previously weighed metal (mild steel) coupon was completely immersed in 250 ml of the test solution in an open beaker. The beaker was inserted into a water bath maintained at 303 K. After every 24 hours, the corrosion product was removed by washing each coupon (withdrawn from the test solution) in a solution containing 50 % NaOH and 100 gL^{-1} of zinc dust. The washed coupon was rinsed in acetone and dried in the air before re-weighing. The difference in weight for a period of 168 h was taken as the total weight loss. From the weight loss results (average of three replicate analysis), the inhibition efficiency (E_{exp}) of the inhibitor, the degree of surface coverage (θ) and the corrosion rate of mild steel (CR) were calculated using Eqs. 1 to 3 respectively [10, 11];

$$E_{exp} = (1 - W_1/W_2) \times 100 \quad (1)$$

$$\theta = 1 - W_1/W_2 \quad (2)$$

$$CR = \Delta W/At \quad (3)$$

where W_1 and W_2 are the weight losses (g) for mild steel in the presence and absence of the inhibitor, θ is the degree of surface coverage of the inhibitor, $\Delta W=W_2-W_1$, A is the area of the mild steel coupon (in cm^2), t is the period of immersion (in hours) and W is the weight loss of mild steel after time, t.

Gasometric method

Gasometric methods were carried out at 303 K as described in the literature [12]. From the volume of hydrogen gas evolved per minute, inhibition efficiencies were calculated using Eq. 4.

$$E_{exp} = \left(1 - \frac{V_{Ht}^1}{V_{Ht}^o}\right) \times 100 \quad (4)$$

where V_{Ht}^1 and V_{Ht}^o are the volumes of H_2 gas evolved at time, 't' for inhibited and uninhibited solutions respectively.

Thermometric method

This was also carried out as reported elsewhere [13]. From the rise in temperature of the system per minute, the reaction number (RN) was calculated using Eq. 5:

$$RN\left(^\circ C\,\mathrm{min}^{-1}\right) = \frac{T_m - T_i}{t} \quad (5)$$

where T_m and T_i are the maximum and initial temperatures respectively and 't' is the time (in minute) taken to reach the maximum temperature. The inhibition efficiency (%I) of the inhibitor was evaluated from percentage reduction in the reaction number as follows:

$$\%I = \frac{RN_{aq} - RN_{wi}}{RN_{aq}} \times 100 \quad (6)$$

where RN_{aq} is the reaction number in the absence of inhibitors (blank solution) and RN_{wi} is the reaction number of the H_2SO_4 containing the inhibitors.

Quantum chemical calculations

Single point energy calculations (for both gas and aqueous phases) were carried out using PM6, PM3, AM1, RM1 and MNDO Hamiltonians in the MOPAC 2008 software for Windows [14]. Calculations were performed using HP laptop having an Intel processor and the following specifications, speed=2.8 GHz; RAM=4 GB and hard disk=250 GB) computer. The following quantum chemical indices were calculated: the energy of the highest occupied molecular orbital (E_{HOMO}), the energy of the lowest unoccupied molecular orbital (E_{LUMO}), the dipole moment (μ), the total energy (TE), the electronic energy (EE), the ionization potential, the cosmo area (cosAr) and the cosmo volume (CosVol). The Muliken and Lowdin charges (q) for nucleophilic and electrophilic attacks were computed using GAMESS computational software [15]. Correlation type and method used for the calculation was MP2 while the basis set was STO-3G.

Statistical analyses were performed using SPSS program version 15.0 for Windows. Non-linear regression analyses were performed by unconstrained sum of squared residuals for loss function and estimation methods of Levenberg-Marquardt using SPSS program version 15.0 for Windows [16].

Results and discussion

Effect of concentration of the inhibitors

Table 1 shows the corrosion rates of mild steel in various media. From the results presented in Table 1, it is evident that the corrosion rates of mild steel in 0.1 M HCl containing various concentrations of oxaldehyde is dependent on the concentration of the oxaldehyde and on temperature. Generally, the corrosion rate decreases with increasing concentration of the additive. Figure 2 shows the variation of the corrosion rates of mild steel in 0.1 M HCl containing various concentrations of benzoin, benzil and pyridoin (as additives). The figure reveals that the corrosion rate of mild steel decreases with increasing concentration of the additives indicating that these compounds inhibited the corrosion of mild steel in HCl solutions. Values of the inhibition efficiencies of benzoin, benzil and pyridoin (calculated from gravimetric, gasometric and thermometric methods) are presented in Table 2. The results obtained, indicate that the inhibition efficiencies of the studied compounds increase with increasing concentration and with increase in temperature. These also indicate that the inhibitors are adsorption inhibitor and that the adsorption of the inhibitors on mild steel surface favors the mechanism of chemical adsorption [17]. For an adsorption inhibitor, the inhibition efficiency tends to increase with an increase in the concentration of the inhibitor as revealed by the present results. Also, for a chemical adsorption mechanism, the inhibition efficiency is expected to increase with increasing temperature [18].

From Table 2, it is also evident that the order for the increase in inhibition efficiency is pyridoin >bezoin> benzil. This implies that pyridoin has the highest inhibition efficiency while benzil has the least.

Values of inhibition efficiency obtained from gasometric and thermometric analysis were found to be comparable to those obtained from gravimetric method. However, results obtained from gasometric and thermometric methods were relatively larger than those obtained from gravimetric results. Therefore, the instantaneous inhibition efficiencies of the studied oxaldehyde are better than their average inhibition efficiencies. This follows from the fact that gasometric and thermometric methods measure instantaneous inhibition efficiency while gravimetric method measures average inhibition efficiency.

Table 1 Corrosion rates of mild steel in 0.1 M HCl containing various concentrations of the studied inhibitors

CR ($gh^{-1}cm^{-2}$)	$C\times10^{-4}$ (M)				
	1	2	3	4	5
Benzoin at 303 K	0.5500	0.4735	0.3724	0.3248	0.2124
Benzoin at 333 K	1.1248	0.9281	0.6760	0.4554	0.2912
Benzil at 303 K	0.9996	0.8958	0.8573	0.7834	0.7120
Benzil at 333 K	1.8887	1.6382	1.4512	1.2807	1.1160
Pyridoin at 303 K	0.3986	0.3249	0.2625	0.1998	0.1596
Pyridoin at 333 K	0.5767	0.4342	0.3515	0.2657	0.2164

CR for the blank=1.25 and 2.75 at 303 and 333 K respectively

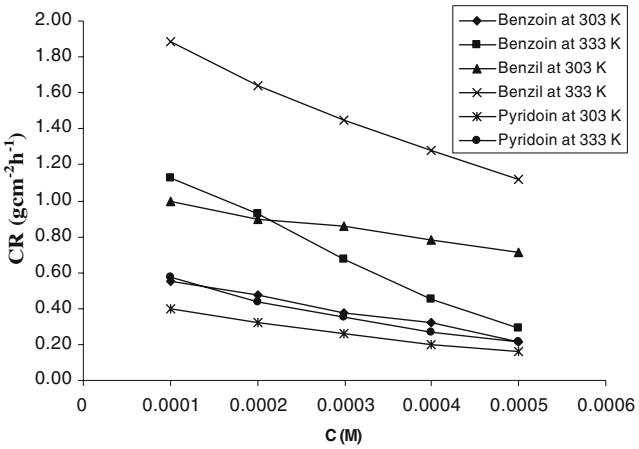

Fig. 2 Variation of the corrosion rate of mild steel with concentration of the studied oxaldehyde at 303 and 333 K

Effect of temperature

The Arrhenius equation was used to calculate the activation energies for the corrosion of mild steel in HCl solutions. The statement of the Arrhenius theory can be expressed as follows: [19],

$$CR = A\ \exp(-E_a/RT), \tag{7}$$

where CR is the corrosion rate of mild steel, A is the Arrhenius or pre-exponential constant, E_a is the activation energy for the reaction, R is the gas constant and T is the temperature in Kelvin. Simplification of Eq. 7 yields Eq. 8,

$$\log(CR) = \log A - E_a/2.303RT. \tag{8}$$

Also, if we assumed that the corrosion rates of mild steel at two temperatures (T_1 and T_2) are CR_1 and CR_2 respectively, then the Arrhenius equation can also be written as follows,

$$\log\frac{CR_2}{CR_1} = \frac{E_a}{2.303R}\left(\frac{1}{T_1} - \frac{1}{T_2}\right). \tag{9}$$

The activation energies calculated from Eq. 9 are presented in Table 3. The results obtained indicated that the values of E_a range from 7.98 to 10.34, 12.58 to 17.81 and from 8.84 to 20.03 kJ mol^{-1} for pyridoin, benzil and benzoin respectively. These values are lower than the value of 22.08 kJ mol^{-1} obtained for the blank and are also lower than the threshold value of 80 kJ mol^{-1} required for the mechanism of chemical adsorption. Therefore, the adsorption of pyridoin, benzoin

Table 2 Inhibition efficiencies of the studied oxaldehyde

Method	Inhibition efficiency (%)	$C\times10^{-4}$ (M)				
		1	2	3	4	5
Gravimetric	Benzoin at 303 K	56.00	62.12	70.21	74.02	83.01
	Benzoin at 333 K	59.10	66.25	75.42	83.44	89.41
	Benzil at 303 K	20.03	28.34	31.42	37.33	43.04
	Benzil at 333 K	31.32	40.43	47.23	53.43	59.42
	Pyridoin at 303 K	68.11	74.01	79.00	84.02	87.23
	Pyridoin at 333 K	79.03	84.21	87.22	90.34	92.13
Gasometric	Benzoin at 303 K	63.40	68.32	74.32	79.21	88.23
	Benzil at 303 K	40.23	56.76	64.32	71.01	76.34
	Pyridoin at 303 K	72.34	74.35	75.43	86.34	91.02
Thermometric	Benzoin at 303 K	59.78	65.09	74.37	78.34	83.98
	Benzil at 303 K	52.38	64.67	68.34	70.09	72.10
	Pyridoin at 303 K	69.93	75.99	78.45	79.30	86.34

and benzil first occurred through the mechanism of physical adsorption. According to Eddy and Ebenso [20], in corrosion inhibition process, physical adsorption inevitably precedes chemisorption and after physical adsorption, the inhibitors are chemically adsorbed on the metal surface.

Thermodynamic/adsorption considerations

The heat of adsorption of the inhibitor was calculated using the following equation [21],

$$Q_{ads} = 2.303R\left[\log\left(\frac{\theta_2}{1-\theta_2}\right) - \log\left(\frac{\theta_1}{1-\theta_1}\right)\right] \times \left(\frac{T_{1X}T_2}{T_2 - T_1}\right) kJmol^{-1}. \quad (10)$$

Calculated values of Q_{ads} are recorded in Table 3. The heats of adsorption were found to range from−64.52 to −77.92 kJ mol^{-1},−49.97 to−73.96 kJ mol^{-1} and from −88.28 to−96.17 kJ mol^{-1} for pyridoin, benzoin and benzil respectively. From these results, it can be stated that the adsorption of the inhibitors on mild steel surface is exothermic.

The free energies for the adsorption of the inhibitors on mild steel surface were calculated using the following relationship [22],

$$\Delta G^0_{ads} = -2.303RT\ \log(55.5K_{ads}), \quad (11)$$

where K=θ/(1-θ)*[C], T is the temperature, R is the gas constant, 55.5 is the molar heat of adsorption of water. Calculated values of the free energies are also presented in

Table 3 Some adsorption parameters for the inhibition of the corrosion of mild steel in 0.1 M HCl by some oxaldehyde

System	E_a ($kJmol^{-1}$)	Q_{ads} ($kJmol^{-1}$)	ΔS_{ads} (kJ/mol)	ΔG^0_{ads}(kJ/mol)
Blank	22.08	–	–	–
1×10^{-4}M benzoin	20.03	2.66	−49.97	−12.48
2×10^{-4}M benzoin	18.84	3.77	−51.52	−11.84
3×10^{-4}M benzoin	16.69	5.53	−54.32	−10.93
4×10^{-4}M benzoin	9.47	11.96	−73.96	−10.45
5×10^{-4}M benzoin	8.84	11.47	−67.85	−9.09
1×10^{-4}M benzil	17.81	12.57	−96.17	−16.57
2×10^{-4}M benzil	16.90	11.33	−88.28	−15.42
3×10^{-4}M benzil	14.74	14.05	−96.04	−15.05
4×10^{-4}M benzil	13.76	13.75	−92.87	−14.39
5×10^{-4}M benzil	12.58	13.88	−91.32	−13.79
1×10^{-4}M pyridoin	10.34	11.91	−76.17	−11.17
2×10^{-4}M pyridoin	8.12	13.16	−77.92	−10.45
3×10^{-4}M pyridoin	8.17	12.49	−73.40	−9.75
4×10^{-4}M pyridoin	7.98	12.08	−69.24	−8.90
5×10^{-4}M pyridoin	8.52	11.30	−64.52	−8.25

Table 3. The results obtained indicate that the adsorption of the inhibitors on mild steel surface is spontaneous.

From the calculated values of the free energy and enthalpy change, the entropies for the adsorption of the inhibitors on mild steel surface were calculated using the Gibb Helmoltz equation (Eq. 12),

$$\Delta S^{o}_{ads} = \left(\Delta G^{o}_{ads} - \Delta H^{o}_{ads}\right)/T. \quad (12)$$

Table 3 also presented the calculated values of entropy changes. From the results obtained, the entropies of adsorption are negative indicating that the adsorption of the inhibitors on mild steel surface is characterized by a decreasing degree of disorderliness.

The adsorption characteristics of the inhibitors were also investigated by fitting data obtained for degrees of surface coverage into different adsorption isotherms including Langmuir, Frumkin, Temkin, El awardy *et al.,* Bockris-Swinkel, Flory-Huggins and Fruendlich adsorption isotherms. The test revealed that the adsorption characteristic of the inhibitors is best described by Langmuir adsorption isotherm. The Langmuir adsorption model relates the degree of surface coverage (θ) to the concentration of an inhibitor as follows [23],

$$\theta = KC \times 1/(1 + KC) \quad (13)$$

where K designates the adsorption equilibrium constant and C is the concentration of the inhibitor in the bulk electrolyte. From the rearrangement of Eqs. 13, 14 and 15 are obtained,

$$1/K + C = C/\theta \quad (14)$$

$$\log(C/\theta) = \log C - \log K. \quad (15)$$

Using Eq. 15, plots of log(C/θ) versus logC are expected to be linear provided the assumptions establishing the Langmuir adsorption isotherm are valid. Figure 3 shows the Langmuir isotherms for the adsorption of pyridoin, benzil and benzoin on mild steel surface. Values of adsorption parameters deduced from the Langmuir adsorption isotherms are presented in Table 4. The data reveal that the slopes and R^2 values for the plots are very close to unity suggesting a strong adherence of the adsorbed inhibitors to the assumptions of Langmuir. The essential features of the Langmuir adsorption isotherm can be expressed in terms of a dimensionless constant called separation factor or equilibrium parameter (K_L) which can be defined as follows:

$$K_L = 1/(1 + KC_0), \quad (16)$$

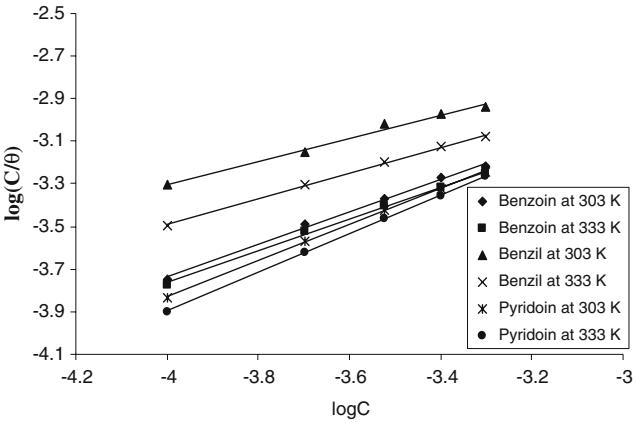

Fig. 3 Langmuir isotherm for the adsorption of the studied oxaldehydes on mild steel surface

where C_0 is the initial concentration of the adsorbate. The significance of Eq. 16 is that when $K_L > 1$, the adsorption is unfavorable; when $0 < K_L < 1$, the adsorption is favorable and when $K_L = 0$, the adsorption is irreversible. Values of K_L obtained in this study were within the range of 0 and unity indicating that the adsorption of the inhibitor on the surface of mild steel is favorable.

It is also significant to note that the values of the equilibrium constant of adsorption (K) obtained from the intercepts of the Langmuir isotherm can be substituted into Eq. 11 in order to obtain the average value of the free energy of adsorption. Values of free energy of adsorption calculated from this option are also shown in Table 4. The values are comparable to those obtained directly from Eq. 11 indicating that Langmuir adsorption isotherm can also be used to predict the spontaneousity of the adsorption process. In this case, the adsorption of the studied oxaldehyde on mild steel surface is spontaneous.

Quantum chemical study

Table 5 shows values of some quantum chemical parameters computed for PM6, PM3, AM1, RM1 and MNDO Hamiltonians (using gas and aqueous phases). The results obtained from gas and aqueous phases are comparable.

Table 4 Langmuir parameters for the adsorption of the studied oxaldehydes on mild steel surface

	T (K)	logK	slope	ΔG^{o}_{ads}(kJ/mol)	R^2
Benzoin	303	0.7643	−0.6800	−6.15	0.9958
	333	0.7388	−0.8049	−5.43	0.9965
Benzil	303	0.5435	−1.1275	−3.55	0.9905
	333	0.6057	−1.0689	−3.89	0.9999
Pyridoin	303	0.8451	−0.4483	−7.49	0.9995
	333	0.9044	−0.2795	−8.47	1.0000

Table 5 Calculated quantum chemical parameters for gas phase (aqueous phase) states of the studied inhibitors

	Models	E_{HOMO} (eV)	E_{LUMO} (eV)	ΔE (eV)	EE (eV)	C-C (eV)	CosAr ($Å^2$)	CosVol ($Å^3$)	μ (Debye)
Pyridoin	PM6	−10.07(−10.50)	−0.91(−1.056)	9.167	−17833.93(−3969.21)	15044.41(1428.64)	234.79(227.27)	254.83(238.64)	4.69(6.92)
	PM3	−10.10(−10.48)	−0.50(−0.54)	9.602	−17601.45(−3687.09)	14853.96(1206.09)	234.79(227.27)	254.83(254.83)	3.97 (5.99)
	AM1	−10.08(−10.33)	−0.40(−0.071)	9.676	−17986.94(−15842.07)	15008.95(13121.21)	234.79(227.27)	254.83(254.83)	4.02(4.69)
	RM1	−9.84(−10.04)	−0.33(0.03)	9.506	−18036.97(−15897.66)	15099.02(13207.53)	234.79(227.27)	254.83(254.83)	4.20(4.96)
	MNDO	−9.87(−10.31)	−0.55(−0.20)	9.322	−18015.35(−15867.18)	15030.90(13140.89)	234.79(227.27)	254.83(254.83)	4.03(4.78)
Benzoin	PM6	−9.66(−10.29)	−0.84(−0.75)	8.816	−15571.16(−3927.87)	13116.85(1470.80)	229.21(232.24)	241.78(247.99)	2.7617(3.73)
	PM3	−9.89(−10.28)	−0.58(−0.37)	9.306	−15299.59(−3651.35)	12874.95(1223.56)	229.21(232.24)	241.78(247.99)	2.4187(3.37)
	AM1	−9.76(−10.22)	−0.41(−0.26)	9.348	−15601.46(−3955.02)	13009.99(1360.00)	229.21(232.24)	241.78(247.99)	2.2329(3.14)
	RM1	−9.63(−9.99)	−0.26(−0.08)	9.366	−15672.65(−4025.84)	13122.16(1472.48)	229.21(232.24)	241.78(247.99)	2.2304(3.24)
	MNDO	−9.85(−10.02)	−0.48(−0.26)	9.368	−15627.07(−3980.78)	13032.42(1381.62)	229.21(232.24)	241.78(247.99)	2.1407(3.09)
Benzil	PM6	−9.61(−9.96)	−1.90(−2.19)	7.717	−14913.02(−3738.80)	12486.89(1312.40)	223.51(223.89)	230.11(231.05)	0.00001(0.002)
	PM3	−10.02(−10.19(	−1.49(−1.65)	8.529	−14638.06(−3463.730	12244.91(1070.42)	223.51(223.89)	230.11(231.05)	0.00001(0.0001)
	AM1	−9.92(−10.10)	−1.32(−1.51)	8.601	−14952.26(−3777.95)	12389.37(1214.88)	223.51(223.89)	230.11(231.05)	0.00001(0.001)
	RM1	−9.86(−10.04)	−1.17(−1.35)	8.694	−15018.73(−3844.40)	12497.32(1322.83)	223.51(223.89)	230.11(231.05)	0.00001(0.001)
	MNDO	−9.99(−10.02)	−1.23(−1.35)	8.763	−14976.38(−3802.04)	12411.18(1236.69)	223.51(223.89)	230.11(231.05)	0.00001(0.001)

According to the frontier molecular orbital theory, the energy of the highest occupied molecular orbital (E_{HOMO}) and that of the lowest unoccupied molecular orbital (E_{LUMO}) are important indices for predicting the reactivity of a chemical species. This is because the adsorption of the inhibitor on the metal surface can be considered on the basis of donor-acceptor interaction between the π-electrons of the inhibitor and a vacant d-orbital of Fe in mild steel [24]. Therefore, increasing values of E_{HOMO} indicates that there is a high tendency for the inhibitor's molecules to donate electrons to the appropriate acceptor molecule, having empty molecular orbital. This will facilitate the adsorption of the inhibitor and ensure better inhibition efficiency by improving the transport process through the adsorbed layer. On the other hand, the value of E_{LUMO} indicates the ability of a molecule to accept an electron. Therefore, the lower the value of E_{LUMO}, the more probable the molecule will accept an electron [25]. The difference between E_{LUMO} and E_{HOMO}, *i.e.*, the energy gap (ΔE) is another index that has been found to have excellent correlations with inhibition efficiencies. The energy gap is related to the hardness and softness of the molecule. Soft molecules are more reactive than hard molecules because the energy to remove electron from the last occupied orbital will be low [26]. Therefore, decreasing value of the ΔE means better inhibition efficiency. Base on the increasing value (absolute values) of the E_{HOMO}, decreasing value of E_{LUMO} and the ΔE, the trend for the variation of the inhibition efficiency is pyridoin >bezoin> benzil. This trend is consistent with experimental data.

Good correlations were also found between the experimental inhibition efficiencies and other quantum chemical parameters, namely, the electronic energy of the molecules (EE), core core repulsion energy (C-C), cosmo area (CosAr), cosmo volume (CosVol) and dipole moment (μ). The inhibition efficiencies of the inhibitors were found to increase with increasing values of C-C, CosAr, CosVol and μ but decrease with increasing value of EE. Figure 4 shows the variation of the experimental inhibition efficiencies with some quantum chemical parameters obtained for PM6 Hamiltonian (for gas phase calculations). Plots for other Hamiltonians and for aqueous phase calculations are not shown because they were similar to those calculated for PM6 Hamiltonian and for gas phase respectively. From Fig. 4, it is evident that there is a good correlation between the quantum chemical parameters and the experimental inhibition efficiencies as indicated by the values of R^2.

Quantitative structure activity relationship (QSAR)

QSAR can be used to correlate the inhibition efficiencies of inhibitors (that are structurally related) to structure parameters (quantum and topological) which can be theoretically

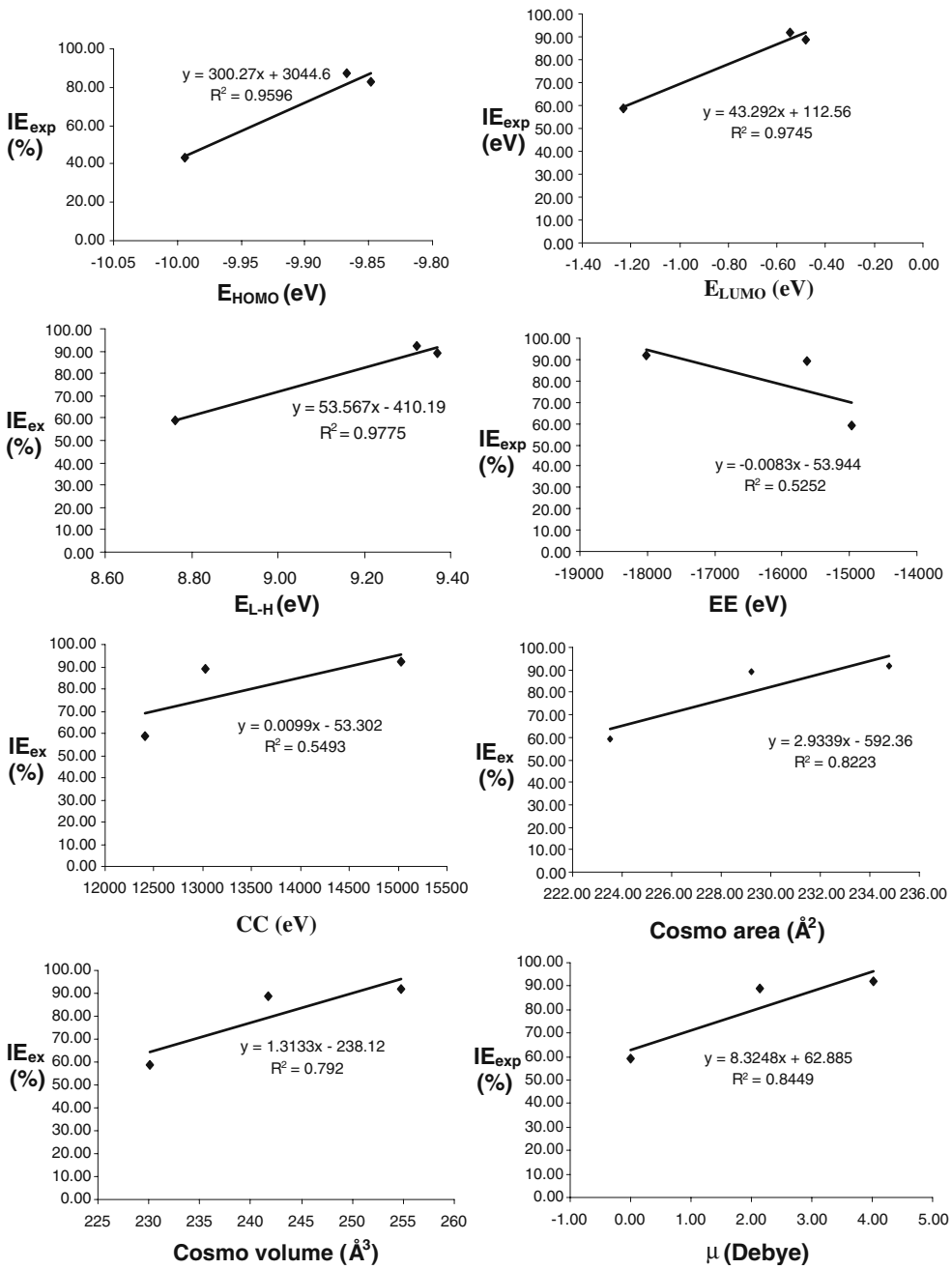

Fig. 4 Variation of experimental inhibition efficiency of the studied oxaldehyde with some quantum chemical parameters

calculated with the ultimate aim of obtaining a molecular design of new corrosion inhibitors. Therefore, QSAR is a useful tool for the development of new corrosion inhibitors because the development of equations for calculating the corrosion inhibition efficiency may lead to a prediction of the efficiency of new inhibitors that are structurally related.

It is significant to note that the adsorption of the inhibitor on mild steel surface is due to the donation of π-electrons by the inhibitor's molecule to the d orbital of Fe in mild steel. However, it is also possible for the electrons from the d orbital of Fe (in mild steel) to be donated to the inhibitor's molecule leading to the formation of a feedback bond. In order to establish the formation of a feedback bond, multiple linear regressions were performed between the experimental inhibition efficiencies and the energy of the frontier molecular orbitals (E_{HOMO} and E_{LUMO}). The regressions yielded Eqs. 17 to 21 for PM6, PM3, AM1, RM1 and MNDO Hamiltonians respectively,

$$E_{exp} = 7.931\,E_{HOMO} + 41.127\,E_{LUMO} + 28.562 \quad (17)$$

$$E_{exp} = 30.386\,E_{HOMO} + 47.564\,E_{LUMO} - 191.127 \quad (18)$$

$$E_{exp} = 961.080\,E_{HOMO} + 234.777\,E_{LUMO} + 9263.020 \quad (19)$$

$$E_{exp} = 12.313\,E_{HOMO} + 33.630\,E_{LUMO} - 1.576 \quad (20)$$

$$E_{exp} = 1.457\,E_{HOMO} + 39.392\,E_{LUMO} - 126.337. \quad (21)$$

The positive values obtained for the coefficients of E_{HOMO} and E_{LUMO} (Eqs. 17 to 21) suggests that the formation of a feedback bond is dependent on the synergistic interaction of E_{LUMO} and E_{HOMO}. On the other hand, when the multiple regression analysis were carried out between the experimental inhibition efficiencies and the calculated quantum chemical parameters (namely, E_{HOMO}, E_{LUMO}, $E_{LUMO\text{-}HOMO}$, TE, EE, C-C, CosAr, CosV, IP and μ), it was not possible to establish a simple relation such as those expressed by Eqs. 17 to 21. This suggests that there exists a complex nature of interactions (between the various quantum chemical parameters) in the corrosion inhibition process.

The linear model for the correlation of experimental inhibition efficiencies with quantum chemical parameters can be approximated as follows, [27]

$$E_{Theor} = Ax_iC + B, \quad (22)$$

where A and B are the regression coefficients determined by regression analysis, x_i is a quantum chemical index characteristic of the molecule i, C is the experimental concentration of the inhibitor. However, application of the above linear approach to the present situation did not give a good correlation between the experimental and theoretical inhibition efficiencies therefore, a non linear model (Eq. 23), which was first proposed by Lukovitis *et al.* [28], for the study of interaction of corrosion inhibitors with metal surface in acidic solutions was used. This model is based on the Langmuir adsorption isotherm and operates on the assumption, which believes that the coverage of the metal surface by the inhibitor's molecule is the primary cause of corrosion inhibition

$$E_{Theor}(\%) = \left\{EQ\backslash f\left(Ax_j + B\right)C_i, 1 + \left(Ax_j + B\right)C_i\right)\right\} \times 100. \quad (23)$$

Using Eq. 23, multiple regressions were performed between the experimental inhibition efficiencies of the inhibitors and the calculated quantum chemical parameters and Eqs. 24 to 28 were obtained for PM6, PM3, AM1, RM1 and MNDO Hamiltonians.

$$E_{Theor} = \frac{(E_{HOMO} + E_{LUMO} + \Delta E + \cos Ar + \cos Vol. + \mu + 109.332) \times C \times 100}{(1 + (E_{HOMO} + E_{LUMO} + \Delta E + \cos Ar + \cos Vol. + \mu + 109.332)^{*}C} \quad (24)$$

$$E_{Theor} = \frac{(E_{HOMO} + E_{LUMO} + \Delta E + \cos Ar + \cos Vol. + \mu + 63.3566) \times C \times 100}{(1 + (E_{HOMO} + E_{LUMO} + \Delta E + \cos Ar + \cos Vol. + \mu + 63.566)^{*}C} \quad (25)$$

Table 6 Theoretical inhibition efficiencies (IE_{Theor}) of the studied oxaldehyde

Inhibitor		Inhibition efficiency (%)				
	C (M)	PM6	PM3	AM1	RM1	MNDO
Pyridoin	1×10^{-4}	77.12	76.90	77.18	77.25	77.21
	2×10^{-4}	87.08	86.94	87.12	87.47	87.14
	3×10^{-4}	91.00	90.90	91.03	91.06	91.04
	4×10^{-4}	93.09	93.01	93.12	93.14	93.13
	5×10^{-4}	94.40	94.33	94.42	94.44	94.42
Benzoin	1×10^{-4}	74.66	74.33	74.61	74.73	74.64
	2×10^{-4}	85.49	85.27	85.46	85.54	85.48
	3×10^{-4}	89.84	89.68	89.81	89.87	89.83
	4×10^{-4}	92.18	92.05	92.46	92.21	92.17
	5×10^{-4}	93.64	93.54	93.63	93.67	93.64
Benzil	1×10^{-4}	73.79	73.43	73.75	73.87	73.78
	2×10^{-4}	84.92	84.68	84.89	84.97	84.91
	3×10^{-4}	89.41	89.24	89.39	89.45	89.84
	4×10^{-4}	91.84	91.70	91.82	91.87	91.84
	5×10^{-4}	93.37	93.25	93.35	93.39	93.36

$$E_{Theor} = \frac{(E_{HOMO} + E_{LUMO} + \Delta E + \cos Ar + \cos Vol. + \mu + 96.000) \times C \times 100}{(1 + (E_{HOMO} + E_{LUMO} + \Delta E + \cos Ar + \cos Vol. + \mu + 96.000)^{*}C} \quad (26)$$

$$E_{Theor} = \frac{(E_{HOMO} + E_{LUMO} + \Delta E + \cos Ar + \cos Vol. + \mu + 209.247) \times C \times 100}{(1 + (E_{HOMO} + E_{LUMO} + \Delta E + \cos Ar + \cos Vol. + \mu + 209.247)^{*}C} \quad (27)$$

$$E_{Theor} = \frac{(E_{HOMO} + E_{LUMO} + \Delta E + \cos Ar + \cos Vol. + \mu + 727.247) \times C \times 100}{(1 + (E_{HOMO} + E_{LUMO} + \Delta E + \cos Ar + \cos Vol. + \mu + 727.247)^{*}C} \quad (28)$$

Values of theoretical inhibition efficiencies calculated from Eqs. 24 to 28 are presented in Table 6 while Fig. 5 shows the variation of the experimental inhibition efficiencies with the theoretical inhibition efficiencies of the

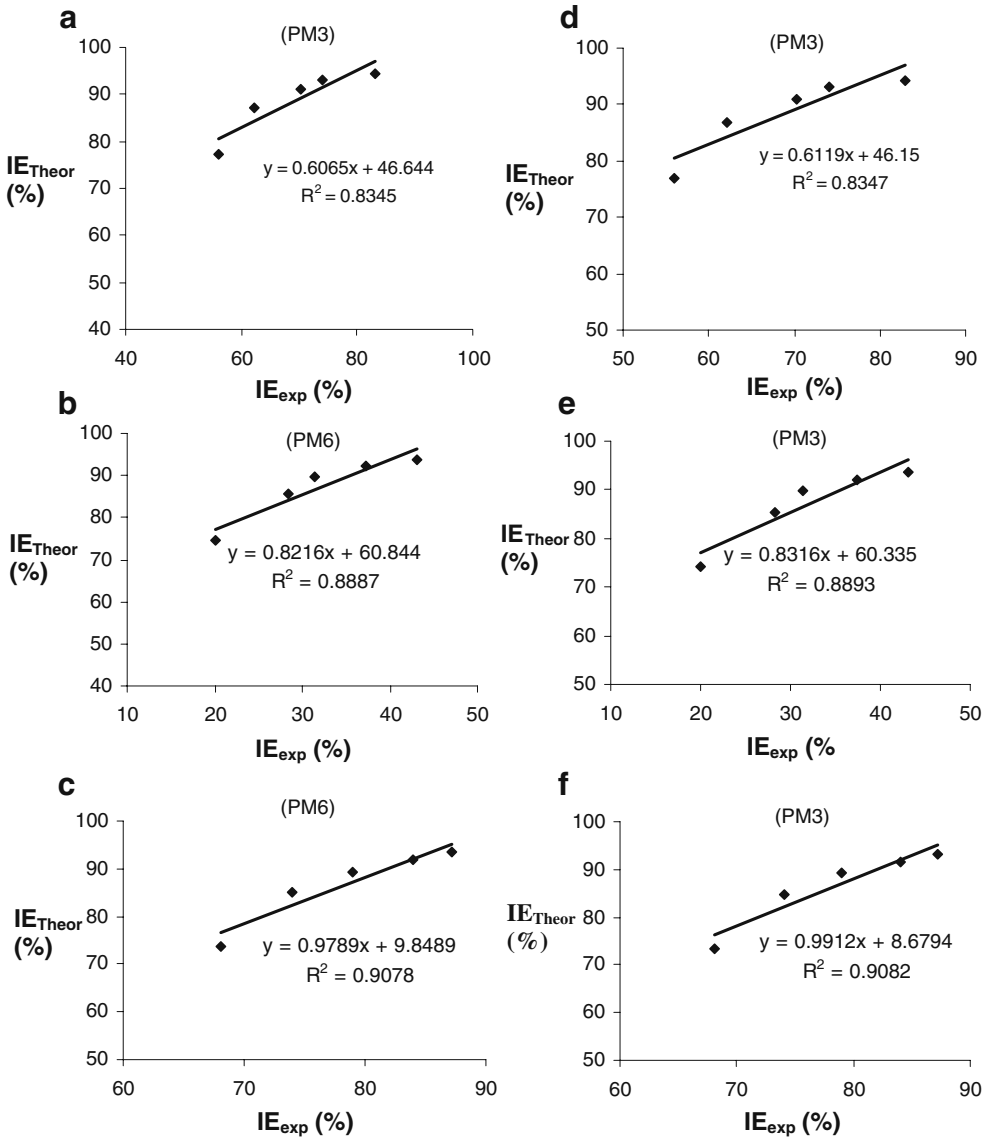

Fig. 5 Variation of experimental inhibition efficiencies of pyridoin (**a** and **e**), benzoin (**b** and **e**) and benzil (**c** and **f**) with the theoretical inhibition efficiencies for the studied oxaldehydes

inhibitors. From the results obtained, it is evident that there is a strong relationship between the experimental and theoretical inhibition efficiencies. Also, for pyridoin, correlations coefficients (r) between experimental and theoretical inhibition efficiencies were 0.9135, 0.9136, 0.9134, 0.9080 and 0.9132 for PM6, PM3, AM1, RM1 and MNDO Hamiltonians respectively. For benzoin, the respective correlation coefficients were 0.9427, 0.9431, 0.9426, 0.9428 and 0.9428 but for benzil r values were 0.9528, 0.9530, 0.9528, 0.9527 and 0.9489 respectively.

DFT study

The principle behind the density functional theory (DFT) is that the energy of a molecule can be determined from the electron density instead of a wave function [29]. DFT principle has been successfully used in the study of corrosion inhibition processes.

The ionization energy (IE) and the electron affinity (EA) of the molecules were calculated using the ground state energies of the respective systems as follows: [30],

$$IE = E_{(N-1)} - E_{(N)} \tag{29}$$

$$EA = E_{(N)} - E_{(N+!)}, \tag{30}$$

where $E_{(N-1)}$, $E_{(N)}$ and $E_{(N+1)}$ are the ground state energies of the system with N-1, N and N+1 electrons respectively. Calculated values of IE and EA are presented in Table 7.

The global hardness of a molecule is one of the parameters that can be used as a reactivity descriptor and is defined as follows [31],

$$\eta = \left(\delta^2 TE/\delta N^2\right)_{V(r)} = {}^{1}/_{2}(\delta\Upsilon/\delta N)_{V(r)}, \tag{31}$$

where Υ is the chemical potential of the electrons, TE is the total energy of the electrons, N is the number of electrons and v(r) is the external potential of the system. The global softness is the inverse of the global hardness. However, in this study, the global hardness and softness were calculated using the finite difference approximation as follows: [32],

$$\eta = \left[\left(E_{(N-1)} - E_{(N)}\right) - \left(E_{(N)} - E_{(N+!)}\right)\right] \tag{32}$$

$$S = 1/\left[\left(E_{(N-1)} - E_{(N)}\right) - \left(E_{(N)} - E_{(N+!)}\right)\right]. \tag{33}$$

Values of η and S calculated from Eqs. 32 and 33 respectively, are also presented in Table 7. As stated earlier, the global hardness and softness are related to the energy gap (ΔE) of the inhibitors. A hard molecule has a large energy gap while a soft molecule has small energy gap implying that a soft molecule is more reactive than a hard molecule.

The fractions of electrons transferred, δ were calculated using the following equations [33],

$$\delta = (\chi_{Fe} - \chi_{inh})/2(\eta_{Fe} + \eta_{inh}), \tag{34}$$

where χ_{Fe} and χ_{inh} are the electronegativity of Fe and the inhibitor respectively. χ=(IP + EA)/2. η_{Fe} and η_{inh} are the

Table 7 Quantum chemical descriptors for the studied oxaldehyde

	Model	E_N (eV)	E_{N-1} (eV)	E_{N+1} (eV)	IE (eV)	EA (eV)	χ (eV)	S (/eV)	η (eV)	δ
Pyridoin	PM6	−2789.52	−2780.28	−2791.11	9.24	1.59	5.41	0.13	7.65	0.10
	PM3	−2747.48	−2737.66	−2748.40	9.82	0.92	5.37	0.11	8.90	0.09
	AM1	−2977.99	−2968.44	−2978.93	9.55	0.94	5.24	0.12	8.61	0.10
	RM1	−2937.95	−2928.25	−2938.83	9.70	0.88	5.29	0.11	8.82	0.10
	MNDO	−2984.44	−2975.12	−2985.52	9.32	1.08	5.20	0.12	8.24	0.11
Benzoin	PM6	−2454.31	−2445.26	−2455.82	9.05	1.51	5.28	0.13	7.54	0.11
	PM3	−2424.64	−2415.15	−2425.74	9.49	1.10	5.29	0.12	8.39	0.10
	AM1	−2591.47	−2582.27	−2592.51	9.2	1.04	5.12	0.12	8.16	0.12
	RM1	−2550.49	−2551.31	−2511.39	9.18	0.90	5.04	0.12	8.28	0.12
	MNDO	−2594.65	−2585.34	−2595.78	9.31	1.13	5.22	0.12	8.18	0.11
Benzil	PM6	−2426.13	−2417.27	−2428.73	8.86	2.60	5.73	0.16	6.26	0.10
	PM3	−2393.15	−2383.89	−2395.22	9.26	2.07	5.66	0.14	7.19	0.09
	AM1	−2562.89	−2553.73	−2564.85	9.16	1.96	5.56	0.14	7.20	0.10
	RM1	−2521.41	−2512.32	−2523.26	9.09	1.85	5.47	0.14	7.24	0.11
	MNDO	−2565.20	−2555.42	−2567.10	9.78	1.90	5.84	0.13	7.88	0.07

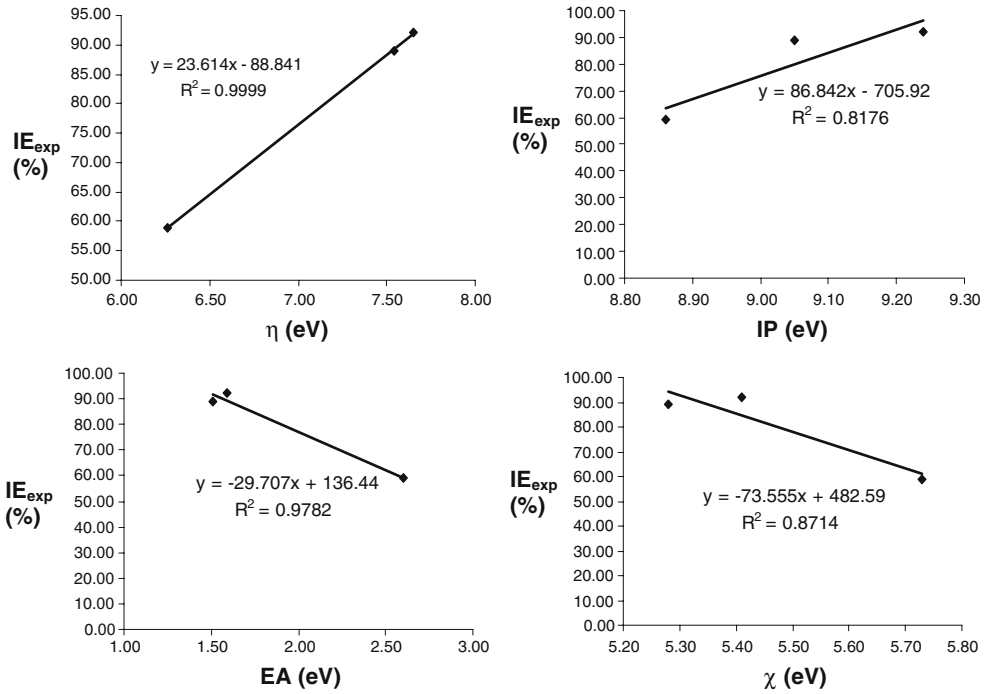

Fig. 6 Variation of experimental inhibition efficiency of the studied oxaldehydes with global hardness, ionization potential, electron affinity and electronegativity

global hardness of Fe and the inhibitor respectively. Validation of Eq. 34 was achieved by adopting the theoretical value of χ_{Fe}=7 ev and η_{Fe}=0 for the computation of δ values. Values of δ obtained from Eq. 34 are also presented in Table 7. The results indicate that there is no significant difference (P>0.05) between the fraction of electrons transferred in each case therefore the concept of using δ values alone may not be significant in predicting the direction of the corrosion inhibition process.

Figure 6 shows the variation of experimental inhibition efficiencies with some quantum chemical descriptors (namely, IE, EA, χ, η and δ). From Fig. 6, it is evident that the R^2 values are very close to unity. Therefore, these quantum chemical descriptors are indices that may show excellent correlation with the corrosion inhibition potentials of a molecule.

Local selectivity

The condensed Fukui and condensed softness were used for the analysis of the local selectivity of the inhibitors. The Fukui and softness functions enable the distinction of each

Table 8 Fukui and global softness indices for nucleophillic and electrophillic attacks in pyridoin calculated from Mulliken (Lowdin) charges (STO-3G)

Atom No	f^+ (|e|)	f^-(|e|)	S^+ (eV|e|)	S^-(eV|e|)
1 C	−3.720(−3.093)	7.794(7.144)	−0.439(−0.365)	0.920(0.843)
2 N	2.907(2.599)	−0.166(0.255)	0.343(0.307)	−0.020(0.030)
3 C	4.113(4.070)	0.035(−0.015)	0.485(0.480)	0.004(−0.002)
4 C	3.958(3.967)	−0.004(0.002)	0.467(0.468)	0.000(0.000)
5 C	3.906(3.527)	−0.018(0.410)	0.461(0.416)	−0.002(0.048)
6 C	0.458(0.688)	3.429(3.230)	0.054(0.081)	0.405(0.381)
7 C	4.072(4.079)	−5.630(−5.414)	0.481(0.481)	−0.664(−0.639)
8 O	1.641(1.734)	−6.235(−6.288)	0.194(0.205)	−0.736(−0.742)
9 C	4.473(3.826)	−8.338(−7.616)	0.528(0.451)	−0.984(−0.899)
10 O	1.683(1.744)	−4.261(−4.369)	0.199(0.206)	−0.503(−0.516)
11 C	−4.406(−3.901)	0.350(−0.094)	−0.520(−0.460)	0.041(−0.011)
12 N	−5.353(−5.257)	4.088(4.0146)	−0.632(−0.620)	0.482(0.474)
13 C	−3.975(−3.989)	7.192(6.700)	−0.469(−0.471)	0.849(0.791)
14 C	−4.110(−4.122)	−0.224(0.228)	−0.485(−0.486)	−0.026(0.027)
15 C	−4.128(−4.088)	−0.003(0.001)	−0.487(−0.482)	0.000(0.000)
16 C	−4.424(−4.066)	0.218(−0.143)	−0.522(−0.480)	0.026(−0.017)

Table 9 Fukui and global softness indices for nucleophillic and electrophillic attacks in benzoin calculated from Mulliken (Lowdin) charges (STO-3G)

Atom No	f^+ (|e|)	f^-(|e|)	S^+ (eV|e|)	S^-(eV|e|)
1 C	−0.0100(−0.0106)	−0.0116(−0.0113)	−0.0012(−0.0013)	−0.0014(−0.0014)
2 C	0.0002(0.0005)	−0.0028(−0.0011)	0.0000(0.0001)	−0.0003(−0.0001)
3 C	0.0125(0.0161)	0.0034(0.0089)	0.0015(0.0020)	0.0004(0.0011)
4 C	−0.0076(−0.0079)	−0.0109(−0.0110)	−0.0009(−0.0010)	−0.0013(−0.0013)
5 C	−0.0102(−0.0113)	−0.0105(−0.0115)	−0.0012(−0.0014)	−0.0013(−0.0014)
6 C	−0.0165(−0.0216)	−0.0146(−0.0192)	−0.0020(−0.0026)	−0.0018(−0.0023)
7 C	−0.0006(0.0006)	−0.0270(−0.0335)	−0.0001(0.0001)	−0.0033(−0.0041)
8 O	−0.0189(−0.0195)	−0.0287(−0.0301)	−0.0023(−0.0024)	−0.0035(−0.0037)
9 C	−0.1687(−0.2063)	−0.0963(−0.1209)	−0.0206(−0.0252)	−0.0117(−0.0148)
10 O	−0.1406(−0.1440)	−0.3025(−0.3375)	−0.0172(−0.0176)	−0.0369(−0.0412)
11 C	−0.0283(−0.0328)	−0.0174(−0.0067)	−0.0035(−0.0040)	−0.0021(−0.0008)
12 C	−0.0521(−0.0657)	−0.0296(−0.0317)	−0.0064(−0.0080)	−0.0036(−0.0039)
13 C	−0.0149(−0.0124)	−0.0187(−0.0183)	−0.0018(−0.0015)	−0.0023(−0.0022)
14 C	−0.0631(−0.0861)	−0.0424(−0.0553)	−0.0077(−0.0105)	−0.0052(−0.0067)
15 C	−0.0189(−0.0179)	−0.0203(−0.0195)	−0.0023(−0.0022)	−0.0025(−0.0024)
16 C	−0.0565(−0.0677)	−0.0424(−0.0466)	−0.0069(−0.0083)	−0.0052(−0.0057)

part of the inhibitor's molecule on the basis of its chemical behavior due to different substituent functional groups. The Fukui function is motivated by the fact that if an electron δ is transferred to an N electron molecule, it will tend to distribute so as to minimize the energy of the resulting N + δ electron system. The resulting change in electron density of the nucleophilic (f^+) and the electrophilic (f^+) Fukui functions can be calculated using the finite difference approximation as follows [34],

$$f^+ = (\delta\rho(r)/\delta N)^+_v = q_{(N+1)} - q_{(N)} \quad (35)$$

$$f^- = (\delta\rho(r)/\delta N)^-_v = q_{(N)} - q_{(N-1)}, \quad (36)$$

where ρ, $q_{(N+1)}$, $q_{(N)}$ and $q_{(N-1)}$ are the density of electron, the Muliken (Lowdin) charge of the atom with N+1, N and N-1 electrons respectively. Calculated values of f^+ and f^-, for pyridoin, benzoin and benzil are presented in Tables 8, 9 and 10 respectively.

Apart from conveying information on the frontier molecular orbital, the Fukui functions also contain information on the change in the molecular shape when electrons are added or removed from the system (*i.e.*, orbital relaxation). From the calculated values of f^+ and f^-, it can be stated that the site for nucleophilic attack would be the place where the value of f^+ is maximum. On the other hand, the site for electrophilic attack is controlled by the value of f^-. Therefore, in pyridoin,

Table 10 Fukui and global softness indices for nucleophillic and electrophillic attacks in benzil calculated from Mulliken (Lowdin) charges (STO-3G)

Atom No	f^+ (|e|)	f^-(|e|)	S^+ (eV|e|)	S^-(eV|e|)
1 C	−0.0140(−0.0153)	−0.0144(−0.0141)	−0.0017(−0.0019)	−0.0018(−0.0017)
2 C	−0.0186(−0.0140)	−0.0218(−0.0280)	−0.0023(−0.0017)	−0.0027(−0.0034)
3 C	−0.0192(−0.0108)	0.0094(0.0212)	−0.0023(−0.0013)	0.0012(0.0026)
4 C	−0.0114(−0.0113)	−0.0274(−0.0314)	−0.0014(−0.0014)	−0.0033(−0.0038)
5 C	−0.0167(−0.0178)	−0.0107(−0.0091)	−0.0020(−0.0022)	−0.0013(−0.0011)
6 C	−0.0184(−0.0221)	−0.0328(−0.0430)	−0.0022(−0.0027)	−0.0040(−0.0052)
7 C	0.0078(0.0065)	−0.0989(−0.1042)	0.0009(0.0008)	−0.0121(−0.0127)
8 C	−0.1030(−0.1350)	−0.1238(−0.1356)	−0.0126(−0.0165)	−0.0151(−0.0165)
9 O	−0.0272(−0.0143)	−0.1575(−0.1677)	−0.0033(−0.0017)	−0.0192(−0.0205)
10 C	−0.0273(−0.0272)	0.0049(0.0146)	−0.0033(−0.0033)	0.0006(0.0018)
11 C	−0.0319(−0.0362)	−0.0241(−0.0307)	−0.0039(−0.0044)	−0.0029(−0.0037)
12 C	−0.0223(−0.0240)	−0.0157(−0.0155)	−0.0027(−0.0029)	−0.0019(−0.0019)
13 C	−0.0371(−0.0461)	−0.0337(−0.0440)	−0.0045(−0.0056)	−0.0041(−0.0054)
14 C	−0.0307(−0.0292)	−0.0115(−0.0099)	−0.0037(−0.0036)	−0.0014(−0.0012)
15 C	−0.0435(−0.0494)	−0.0297(−0.0334)	−0.0053(−0.0060)	−0.0036(−0.0041)
16 O	−0.2796(−0.3120)	−0.1796(−0.1940)	−0.0341(−0.0381)	−0.0219(−0.0237)

the site for nucleophilic and electrophilic attacks are in the carbonyl bond (*i.e.*, C(9)-O(10)) and alkene-pyridinic bond (*i.e.*, C(1)-N(3). In benzoin, the sites fro nucleophilic and electrophilic attacks are in the phenyl alkene (*i.e.*, C3). However, in benzil, the sites for nucleophilic and electrophilic attacks are in the carbonyl functional group (*i.e.*, C(7)-O(16) and in the phenyl alkene (C (3)) respectively.

Application of the molecular orbital theory reveals that additional electrons would occupy the lowest unoccupied molecular orbital (LUMO) whereas upon ionization, electrons would be removed from the highest occupied molecular orbital (HOMO). Consequently, the Fukui functions (f^+ and f^-) of a given molecule are expected to be related to the LUMO and HOMO of that molecule. Figure 7 shows the HOMO and LUMO molecular orbital diagrams of pyridoin, benzoin and benzil. The figure clearly indicates that the information generated by the Fukui function are similar to those revealed by the LUMO and HOMO diagrams.

The local softness, s for an atom is the product of the condensed Fukui function (f) and the global softness (S) and can be expressed as follows [35],

$$s^+ = (f^+)S \tag{37}$$

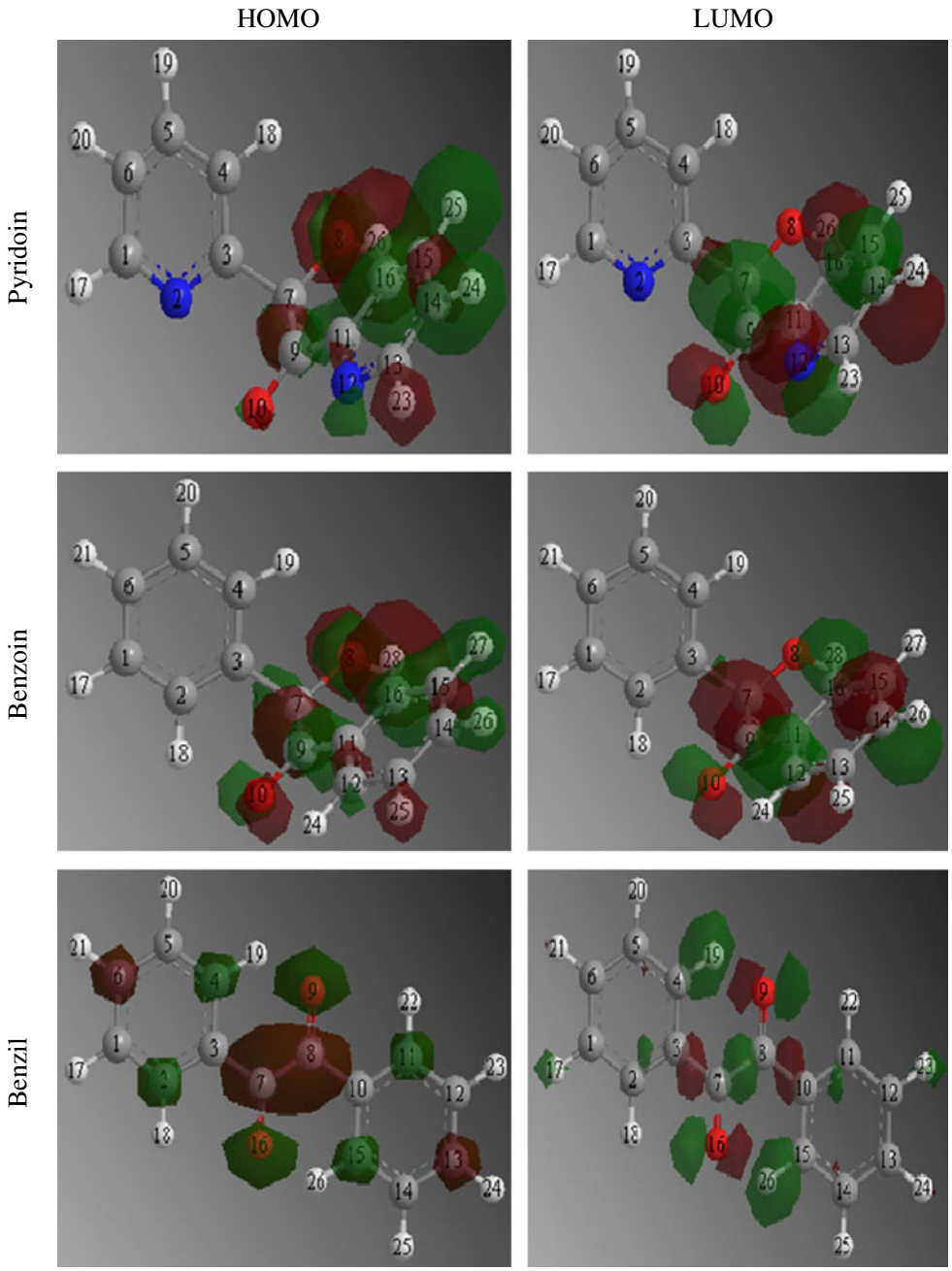

Fig. 7 Molecular orbital of pyridoin, benzoin and benzil showing the HOMO and the LUMO

$$s^- = (f^-)S. \quad (38)$$

According to the HSAB principle, a reaction between an acid A and a base B will be favored when the global softness difference ΔS, defined in Eq. 39 is minimal. This is obtained through optimization of the covalent contribution of the interaction energy, thereby neglecting other effects such as polarization

$$\Delta S = S_A - S_B. \quad (39)$$

Calculated values of the condensed local softness are also presented in Tables 8, 9 and 10. From the results obtained, it is evident that the sites for nucleophilic and electrophilic attacks are in the atoms where the softness indices are the lowest.

Conclusions

Pyridoin, benzoin and benzil are good adsorption inhibitors for the corrosion of mild steel in HCl solutions. The adsorption of the inhibitors on mild steel proceeded supports the mechanism of physical adsorption. The adsorption of the inhibitors is exothermic, spontaneous and can best be described by Langmuir adsorption isotherm. QSAR, DFT and quantum chemical studies can adequately be used to study the inhibition potentials of oxaldehydes for mild steel corrosion in HCl solutions.

Acknowledgments The authors are grateful to Dr. Stanislav R. Stayanov of the Institute of Nanotechnology, National Research Council of Canada for his leading in the principles and application of computational chemistry.

References

1. Abdallah M (2002) Corros Sci 44:717–728
2. Abiola OK, Oforka NC, Ebenso EE, Nwinuka NM (2007) Anti-Corros Methods Mater 54(4):219–224
3. Acharya S, Upadhyay SN (2004) Trans Indian Inst Met 57 (3):297–306
4. Agrawal YK, Talati JD, Shah MD, Desai MN, Shah NK (2003) Corros Sci 46:633–651
5. Ebenso EE, Eddy NO, Odiongenyi AO (2009) Port Electrochim Acta 27(1):13–22
6. Odoemelam SA, Ogoko EC, Ita BI, Eddy NO (2009) Port Electrochim Acta 27(1):57–68
7. Yurt A, Bereket G, Ogretir C (2005) J Mol Struct THEOCHEM 725:215–221
8. Bentiss F, Lebrini M, Lagrenee M, Traisnel M, Elfarouk A, Vezin H (2007) Electrochim Acta 52:6865–6872
9. Gao G, Liang C (2007) Electrochim Acta 52:4554–4559
10. Eddy NO, Ibok, UJ, Ebenso EE (2009) J Appl Electrochem, doi:10.1007/s10800-009-0015-z
11. Abdallah M (2004) Corros Sci 46:1981–1996
12. Eddy NO, Odoemelam SA, Odiongenyi AO (2009) J Appl Electrochem 39(6):849–857
13. Eddy NO, Odoemelam SA (2009) Pigm Resin Technol 38(2):111–115
14. MOPAC2009, Stewart JP, Stewart Computational Chemistry, Version 9.069 W. web: http://OpenMOPAC.net
15. Schmidt MW, Baldridge KK, Boatz JA, Elbert ST, Gorson MS, Jensen JH, Koseki S, Matsunage N, Nguyen KA, Su SJ, Windus TS, Dupius M, Montgomery JA (2008) GAMES Version 11. From Iowa State University. J Comput Chem 14:1347–1363
16. http://www.spss.com/
17. Eddy NO (2009) Molecular simulation. doi:10.1080/08927020903483270
18. Sahin M, Gece G, Karci F, Bilgic S (2008) J Appl Electrochem 38:809–815
19. Eddy NO, Odoemelam SA, Odiongenyi AO (2009) Green Chem Lett Rev 2(2):111–119
20. Eddy NO, Ebenso, EE (2009) J Mol Model. doi:10.1007/S00894-0090635-6
21. Eddy NO (2009) Port Electrochim Acta 27(5):579–589
22. Ashassi-Sorkhabi H, Shaabani B, Seifzadeh D (2005) Electrochim Acta 50:3446–3452
23. Eddy NO, Ibok UJ, Ebenso EE, Ahmed E, El Sayed HE (2009) J Mol Model 15(9):1085–1092
24. Bentiss F, Bouanis M, Mernari B, Traisnel M, Vezin H, Lagrenee M (2007) Appl Surf Sci 253:3696–3704
25. Khaled KF, Babic-Samardzija K, Hackerman N (2005) Electrochim Acta 50:2515–2520
26. Bentiss, Traisnel M, Chaibi N, Mernari B, Vezin H, Lagrenee M (2002) Corros Sci 44:2271–2289
27. Arslan T, Kandemirli F, Ebenso EE, Love I, Alemu H (2009) Corros Sci 51:35–47
28. Lukovitis I, Bako I, Shaban A, Kalman E (1998) Electrochem Acta 43:131–135
29. Young DC (2001) Computational chemistry. A practical guide for applying techniques to real-world problems. Wiley, New York, p 42
30. Stayanov SR, Kral P (2006) J Phys Chem B 110:21480–21486
31. Stayanov SR, Gusarov S, Kovalenko A (2008) Mol Simul 34 (10):10–15
32. Fang J, Li J (2002) J Mol Struct THEOCHEM 593:179–185
33. Wang H, Wang X, Wang H, Wang L, Liu A (2007) J Mol Model 13:147–153
34. Fukui K, Yonezawa T, Shingu H (1952) J Chem Phys 20:722–725
35. Stayanov SR, Gusarov S, Kunznicki SM, Kovalenko A (2008) J Phys Chem C 112:6794–6810